AIAA-99-1719

A NEW PNEUMATIC ACTUATOR AND ITS USE IN AIRDROP APPLICATIONS

Glen Brown* and Roy Haggard†
Vertigo, Inc.
P.O. Box 117
Lake Elsinore, CA 92531-0117

Richard Benney‡ and Nicholas Rosato§
US Army Soldier & Biological Chemical Command
Soldier Systems Center
Natick, MA 01760-5017

ABSTRACT

Most recovery systems could be improved if they used a smaller main parachute, yet landed with a slower descent velocity. Depending on the application, benefits could include reduced system weight, faster opening, lower opening force, opening at higher airspeeds, reduced impact loads, and reduced impact attenuation material bulk and weight. This paper describes a device that reduces parachute landing velocity by rapidly retracting the payload toward the parachute shortly before impact.

Newly developed flexible composite technology makes compact and highly efficient long-stroke actuators for parachute retraction possible. These actuators are slender flexible tubes with a mechanical attachment at each end and a pneumatic fitting at one end. Prior to pressurization, the actuator is flexible and can be packed with the parachute. When pressure is applied through the end fitting, the actuator contracts strongly, providing a force useful for a variety of applications. The name "Pneumatic Muscle Actuator" (PMA) is descriptive of this device.

This paper discusses parachute retraction and the use of PMAs for the soft landing of cargo and vehicles. Parachute retraction soft landing is currently being studied at the US Army Soldier & Biological Chemical Command, Soldier Systems Center where continuing analysis and tests are showing this concept's potential.

HISTORICAL BACKGROUND

A contracting braided tube device was known and described at least as far back as a 1940 patent by Pierce (US 2,211,478). The device described was actually related to mining operations, rather than airdrop, but shows the principle of the pneumatic muscle quite clearly (Figure 1).

A pneumatic muscle for retraction soft landing was described in 1949 by DeHaven (US 2,483,088) (Figure 2). DeHaven's invention was remarkable, first, in that it came in a time before high tenacity fibers, and second, in that it described such details as the pyrotechnic gas generator and closure of the braided tube in ways that can scarcely be faulted today.

---

* Director of Engineering, Senior Member
† Engineering Manager, AIAA Member
‡ Aerospace Engineer, Senior Member
§ Research Mechanical Engineer

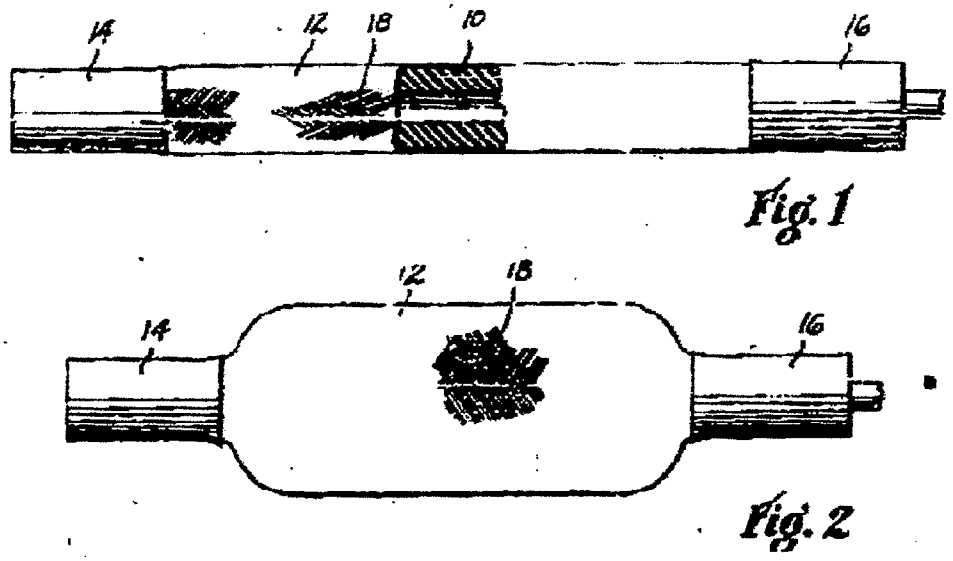

Figure 1 Pierce's Patent Drawing

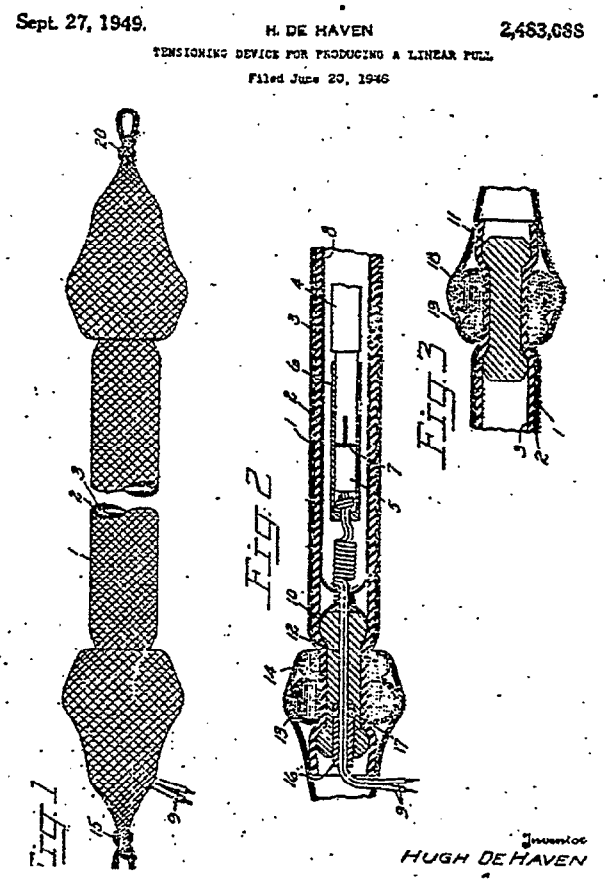

Figure 2 DeHaven's Patent Drawing

The more recent association of the pneumatic muscle actuator with retraction soft landing stems from soft landing research at Natick[1] and a concept for pneumatic parafoil and parachute steering being developed at Vertigo[2]. This paper discusses the characteristics of PMAs as they apply to soft landing and progresses toward implementing a practical soft landing system.

SOFT LANDING SYSTEM DESCRIPTION

A soft landing airdrop system consists of a payload, parachute(s) and the retraction device. The payload and the parachute can be completely standard, inventory items. In the example of an airdropped HMMWV (Figure 3) we assume a payload weight of approximately 10,000 lb. and the use of two G-11 parachutes. This is an interesting example and an application with high potential payoff because this combination descends at approximately 28 ft/sec, but could land at 10 ft/sec or less eliminating the need for impact attenuation material.

A pneumatic muscle actuator (PMA) used as a retraction device consists of a braided fiber tube, a gas barrier liner, one end closure with a mechanical load attachment, and one end with a mechanical load attachment, a pyrotechnic gas generator and a ground proximity sensing initiator.

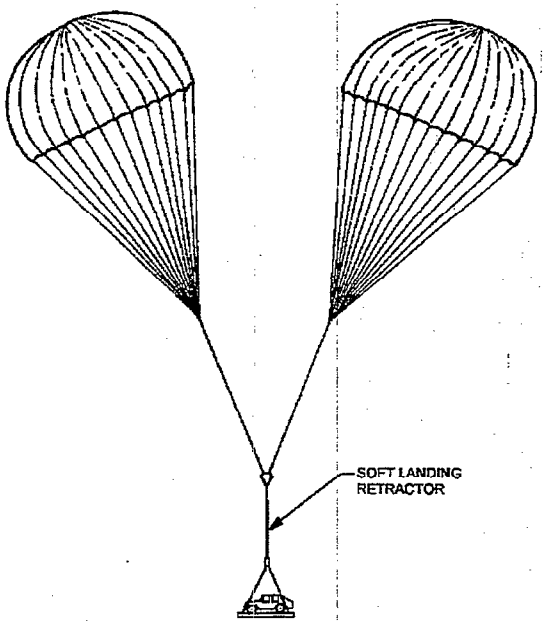

Figure 3 HMWWV Soft Landing System

PMA FORCE EQUATION

The actuator is constructed as a tube of braided fibers. The braid includes only bias fibers, which allows the tube to change length in response to force and pressure changes. In operation, the actuator also changes diameter and fiber bias angle whenever length changes in response to pressure or applied load. (Bias angle is measured from lines parallel to the tube axis.) Length and diameter are related to bias angle by:

$$\frac{d}{d_o} = \frac{\sin\beta}{\sin\beta_o}, \text{ and}$$

$$\frac{l}{l_o} = \frac{\cos\beta}{\cos\beta_o}.$$

The force generated by a pneumatic muscle actuator can be found by summing the axial component of tension in the fibers and subtracting the axial pressure reaction. It is found that at small angles the tension component summation far exceeds the pressure reaction, producing a net tension, or contraction force. However, it is easier to solve for the force by the principle of virtual work as is done below.

Setting the work done by an infinitesimal change in length equal to the change in the internal energy of the gas contained in the system,

$$F \bullet dl = P \bullet dV$$

which leads to the force equation:

$$F = P\frac{dV}{dl}$$

The derivative of volume with respect to length is found conveniently by defining a unit length as the axial length that one fiber of the braid travels as it traverses one circumference of the cylinder. If the braid is slit and laid flat that fiber forms the hypotenuse of a right triangle with sides πd and l, having a length s.

$$s^2 = \pi^2 d^2 + l^2$$

$$l = \frac{\pi d}{\tan\beta}$$

The volume of the unit length cylinder is:

$$V = \frac{\pi}{4} d^2 l$$

$$= \frac{1}{4\pi} l(s^2 - l^2)$$

And, the volume derivative is:

$$\frac{dV}{dl} = \frac{1}{4\pi}[(s^2 - l^2) - 2l^2]$$

$$= \frac{1}{4\pi}[s^2 - 3l^2]$$

$$= \frac{1}{4\pi}\left[\pi^2 d^2 + \frac{\pi^2 d^2}{\tan^2\beta} - 3\frac{\pi^2 d^2}{\tan^2\beta}\right]$$

$$= \frac{\pi}{4} d^2\left[1 - \frac{2}{\tan^2\beta}\right]$$

The contraction force is therefore:

$$F = \frac{\pi}{4} P d^2 \left[1 - \frac{2}{\tan^2 \beta} \right]$$

The equation can be written as a force coefficient that compares the force generated to the force produced by a pneumatic cylinder of the same diameter:

$$C_T = \frac{F}{\frac{\pi}{4} P d_o^2}$$

$$= \left(\frac{d}{d_o} \right)^2 \left[1 - \frac{2}{\tan^2 \beta} \right]$$

or in terms of length:

$$= \left(\frac{l}{l_o} \right)^2 \frac{\tan^2 \beta}{\tan^2 \beta_o} \left[1 - \frac{2}{\tan^2 \beta} \right]$$

A more useful form of this equation in terms of a single variable is

$$C_T = \left(\frac{\cos \beta}{\cos \beta_o} \right)^2 \left(\frac{\tan \beta}{\tan \beta_o} \right)^2 \left[1 - \frac{2}{\tan^2 \beta} \right]$$

$$C_T = \frac{[\sin^2 \beta - 2 \cos^2 \beta]}{\sin^2 \beta_o}$$

Since dynamics of the retraction system are more conveniently calculated with the length variable, use

$$\beta = \cos^{-1} \left(\frac{l}{l_o} \cos \beta_o \right)$$

to arrive at...

$$C_T = \frac{\left[\sin^2 \left(\cos^{-1} \left(\frac{l}{l_o} \cos \beta_o \right) \right) - 2 \cos^2 \left(\cos^{-1} \left(\frac{l}{l_o} \cos \beta_o \right) \right) \right]}{\sin^2 \beta_o}$$

Maximum stroke and force is produced by an actuator having a small initial bias angle. The graph found in Figure 4 was calculated for a pneumatic muscle actuator having an initial bias angle of 15 degrees. Note the remarkably high tension coefficient, starting at well over twenty, and the useful contraction of nearly 40 percent.

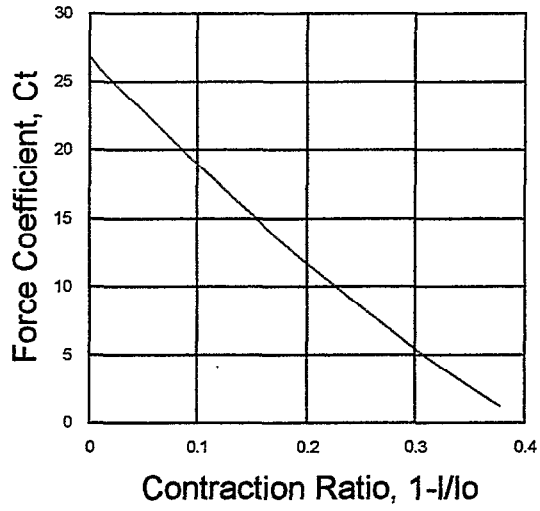

Figure 4 PMA Force Curve from Theory

Actual force generated is reduced by any resistance of the individual fiber bundles to pivoting on one another with bias angle changes and by the expansion of the stretched elastomeric gas barrier inside the braided tube. The actual force is also reduced by the fixed end fittings, which are not allowed to expand in diameter as does the rest of the tube. The following section compares static force measurements with this simplified estimate.

STATIC TESTING

Prototype fabrication and testing were used to validate the predicted PMA performance. The graph contained in Figure 5 shows the force generated in a 1.05 inch diameter, 34 inch long PMA.

Actual force generated is less than the theoretical prediction. This is to be expected from end effects, liner elasticity and fiber-fiber friction. The ratio of actual to predicted force is also plotted. Over the operating range, the efficiency of the muscle is in the range 85% to 65%, with the highest efficiency during initial contraction.

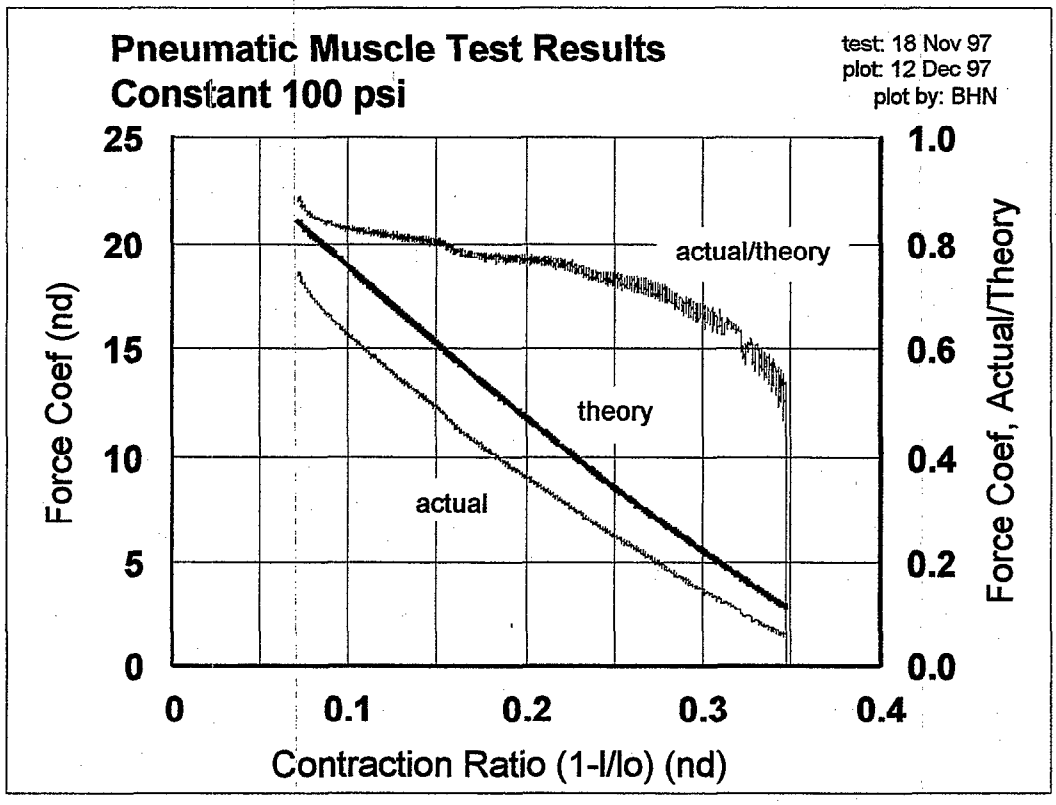

Figure 5 Measured Force Compared to Theory

PERFORMANCE COMPARISONS

How do PMAs compare to other devices capable of the same action? Figure 6 illustrates several comparisons.

Inflating PMAs requires the use of either stored compressed gas or a pyrotechnic gas generator. The first bar graph compares an advanced lead-acid battery with a hot pyrotechnically generated gas (1000°F) and a compressed gas stored at 59°F. When the work required is of short enough duration to allow the use of a single discharge of hot gas, the pyrotechnic generator is superior. For multiple actuator strokes over a long period of time, the lead-acid battery is superior when compared to compressed gas storage.

Specific power is compared in the second bar graph of Figure 6. A truck winch is used as an example of an electromechanical device. The PMA is far superior because increasing the power of a PMA requires only increasing the size of the flow passage, which does not increase the weight of the PMA. Increasing the power of an electric motor requires additional iron and copper in direct proportion to the amount of power required. This comparison is applicable to parachute retraction, parafoil steering and parafoil flare.

The third comparison shown in Figure 6 is for the specific impulse, which is most useful for soft landing retraction. The PMA is compared to a solid propellant retro-rocket for which a good specific impulse would be approximately 280 seconds. Various simulations of PMA retraction processes indicate a specific impulse of approximately 1400 seconds, which represents a considerable improvement.

SOFT LANDING PERFORMANCE

Krainski[1] has previously reported on the simulation of a soft landing retractor implemented with a mechanically stroke-amplified pneumatic cylinder. The primary differences in the simulation of this system when compared to Krainski's work are in the number of rigid bodies and the flow model. Because the majority of the mass of the device moves with either the payload or the parachute, a 2-body simulation is adequate for the pneumatic muscle. Krainski uses a volume of stored gas that communicates with no flow restriction to the pneumatic cylinder at the time of initiation, while the PMA system under investigation uses choked flow from a hot, high pressure source.

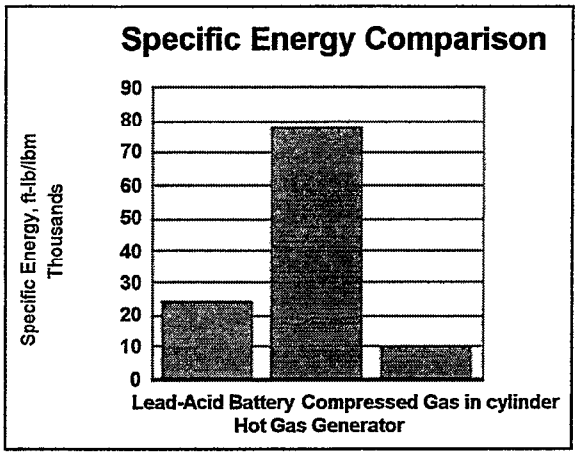

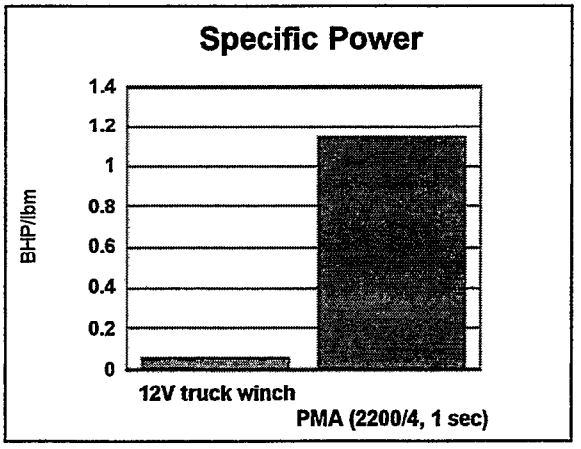

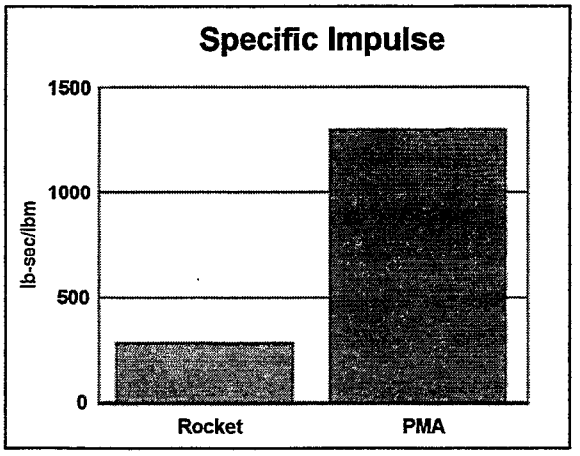

Figure 6 PMA Performance Comparisons

A simple simulation was written in spreadsheet format to explore the design variables and performance. The integration method is stepwise constant acceleration, using the forces of the previous time step to calculate the displacement and velocity. This allows calculation in a single pass through the sheet, is accurate for slowly varying forces, and can be verified by looking at the sensitivity of the result to the time step value.

The graphs in Figure 7 show performance estimates for a 14 ft long, 6.0 inch diameter PMA retracting a 10,000 lbm payload. A gas generator burn of 6.0 lb/sec for 0.20 seconds produces a peak acceleration of 8.8 g and a ΔV of 18.8 ft/sec.

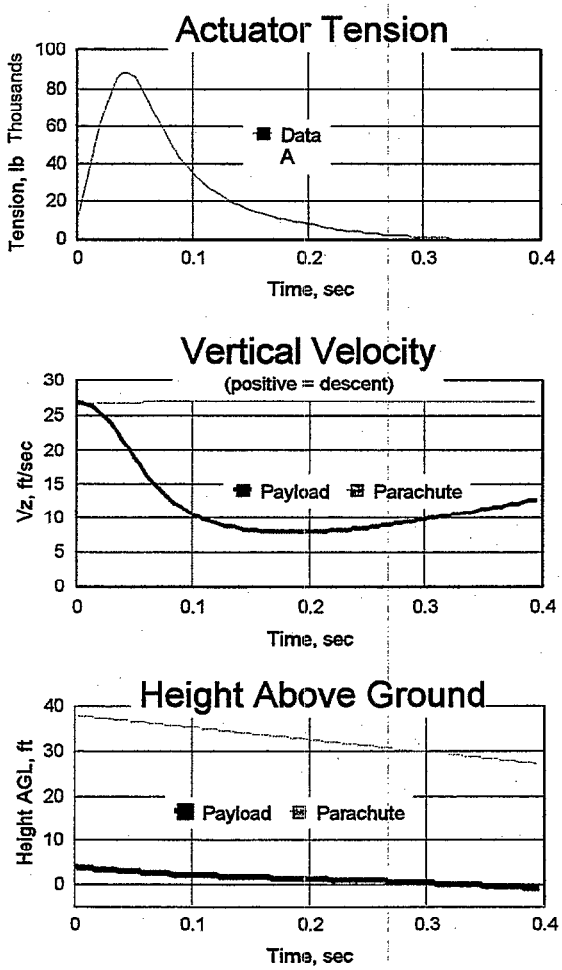

Figure 7 Calculated Soft Landing of 10,000 lbm Payload

With an initial descend rate of 26.7 ft/sec (under two G-11 parachutes), descent rate is reduced to less than 10 ft/sec for a period of 0.21 seconds. If the trigger initiates at between 3.7 and 1.9 (2.8 and 0.9) feet above the ground, the resulting impact will be less than 10 ft/sec.

DYNAMIC TESTING

A dynamic test was also conducted using a 300 lb torso dummy and a 1.05 inch diameter, 16 ft long PMA. The test setup is shown in the photo of Figure 8, with the dummy at the top of its trajectory.

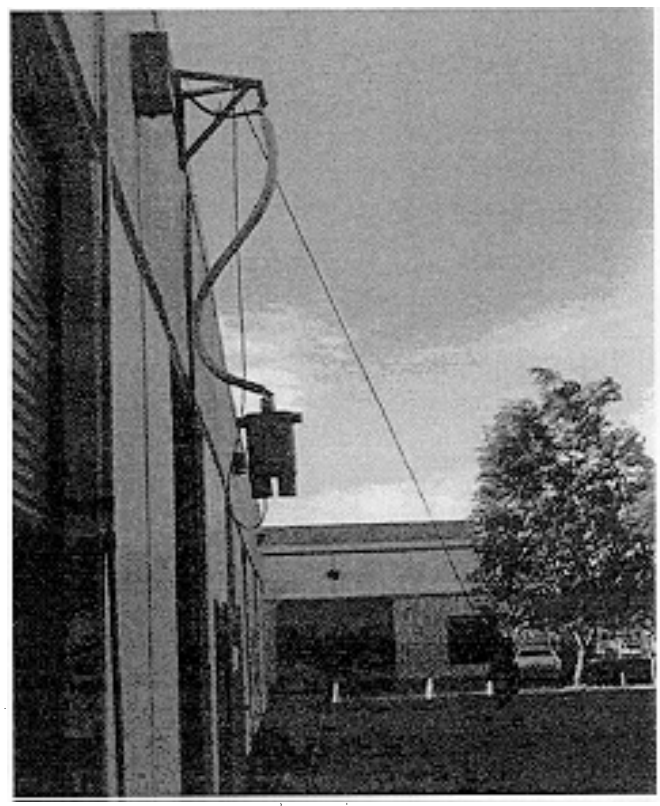

Figure 8 Dynamic Test with 300 lbm

The dummy was lifted off the ground by rapid inflation from a reservoir tank that had initial pressures varying from 25 to 150 psig. The flow into the PMA was slowed by pipe losses compared to an integrated gas generator, but the contraction was still strong and rapid. PMA tension loads were measured and are plotted in the graph of Figure 9.

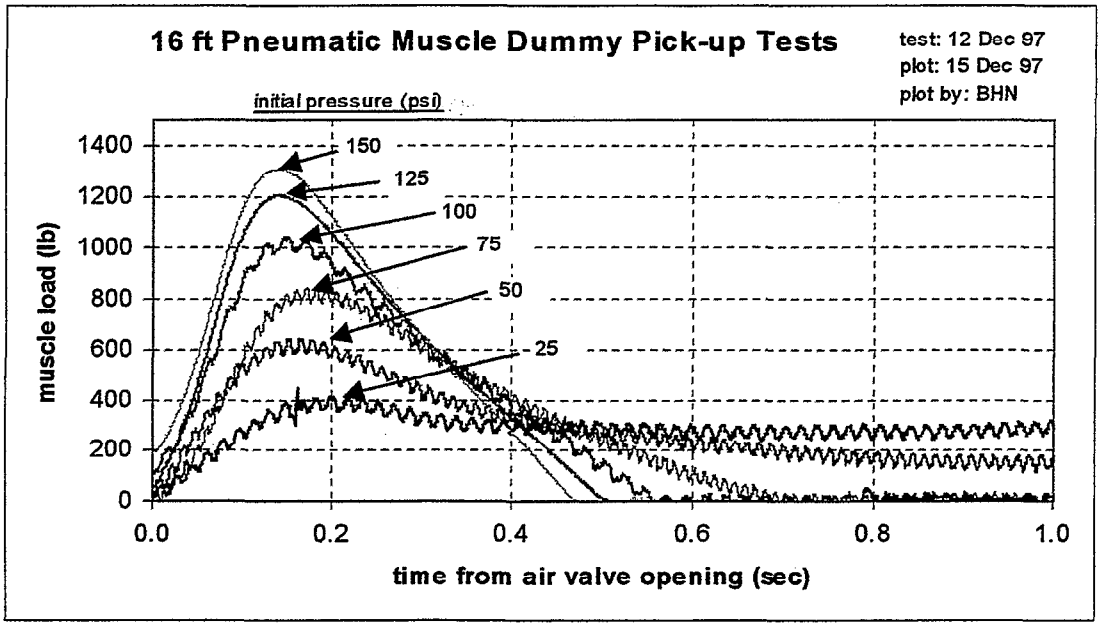

Figure 9 Force Curves from Dynamic Tests

FINITE ELEMENT MODELING OF PMAS

The ability to predict PMA performance and behavior with a high fidelity model is desirable for the prediction of forces applied to the load, the effects of end caps on performance, varying material properties, static shapes under loads, force histories, and other real effects not included in the basic force equation.

A finite-element-based structural dynamic (SD) model is utilized to model PMA statics and dynamics. The software known as "TENSION9" has many features that make it especially useful for modeling fiber reinforced membrane structures like PMAs. The TENSION9 theory with airdrop system modeling examples are described in detail in other works[3,4]. TENSION9 is also being applied to model controllable round and cross canopy airdrop systems where a PMA control actuator could deform the canopy system and produce glide[6]. The code is coupled to a pre and post processing software suite written in Matlab$_{TM}$. A module to "build" PMA models has been constructed for easy assembly of PMA "unit cells" and duplication of the unit cells into PMA structures.

In addition, the TENSION9 software has recently added a user-defined, rotated-coordinate-system feature which allows the user to build a single column of PMA unit cells to model a "sliver" of the PMA's circumference in detail down to every fiber in the braid but at significantly lower computational cost. Simulations with this option are ongoing and will not be reported in detail here. A one-inch diameter, 15-foot long, quarter-symmetry PMA model is presented here as an example (Figure 10).

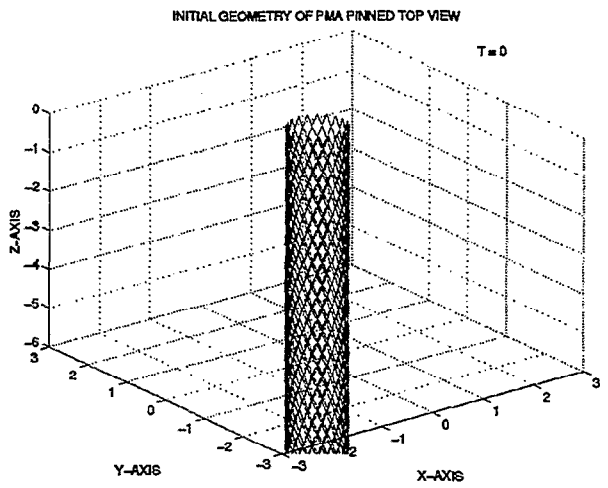

Figure 10 FEA model of PMA

For this 1 inch diameter model, the overall length is 15 feet (close to the pull up experiments) and the weight applied to the base is equivalent to a total payload weight of 250 pounds. In this case, the model's circumference contains 5 unit cells while the length is 307 unit cells long. The total model contains 1535 unit cells. This equates to 3,383 node points and 12,286 elements (6,140 two-noded cables, 6,140 3-noded membranes and

6 concentrated mass elements). The model is initially unstretched and both an internal pressure of five psi and gravity are "turned on" at the start of the simulation. The pressure is increased from five psi to 50 psi over the first 0.1 seconds and then held at 50 psi for the duration of the simulation. A small quantity of mass-proportional damping is used throughout the simulation. This is used to assist in numerical stability and simulate a small amount of damping in the fiber braid material which may be modeled with two-noded dampers in the future.

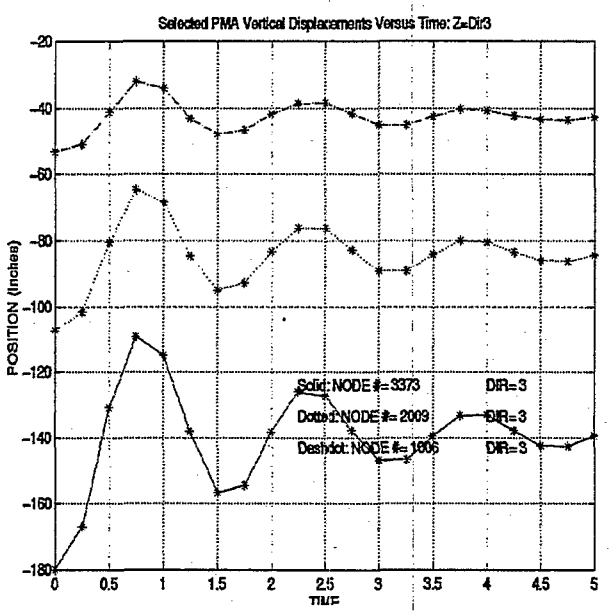

Figure 11 FEA dynamic results

Additional features that may be added include kink and/or fold elements applied to model the friction effects of the membrane/fiber and fiber/fiber interactions. In addition, utilization of a membrane wrinkling model could be applied to the inner liner membrane (see ref 5 for more information on specialized features of TENSION9). The simulation is run for five seconds in real time.

The time history of a payload node and velocity in the vertical direction are shown in Figure 11. The simulation predicts a damped oscillation as expected with the first "peak" being of primary interest in this simulation. The model predicts a payload vertical pull of nearly six feet (over 70 inches) during the first peak. The other nodes follow the same trend as expected and witnessed during the real tests. The velocity of the payload reaches well over 11 feet/second (over 130 inches/second).

The end cap shape at the top of the PMA is shown in Figure 12 at a time of five seconds (the final time of the simulation). The shape appears as expected based on static tests conducted with the one inch diameter PMA.

These results are relatively close to those obtained experimentally considering the crude material properties utilized and the simplified loading applied. The model also predicts the accelerations (G-forces) applied to the payload, the time dependent forces experienced by the fibers in the model and the stresses experienced in the liner membrane. The model has many assumptions including: a) The membrane and fibers are attached to each other and relative sliding is not included, b) The fiber braids are "pinned" to each other throughout the simulation, c) For the symmetry models, only symmetric effects are modeled (full 3D models can be used but they require more computational time), d) The frictional effects are approximated, e) The applied pressure is linearly ramped to a constant level and is kept constant during the oscillations, f) The material properties are approximated and assumed to be linearly elastic (the fiber Young's Modulus has a significant effect on results).

Continued simulation of PMAs is ongoing. A "wedge" model utilizing higher order PMA unit cells has been constructed to model the large six inch diameter PMA pull tests and static tests.

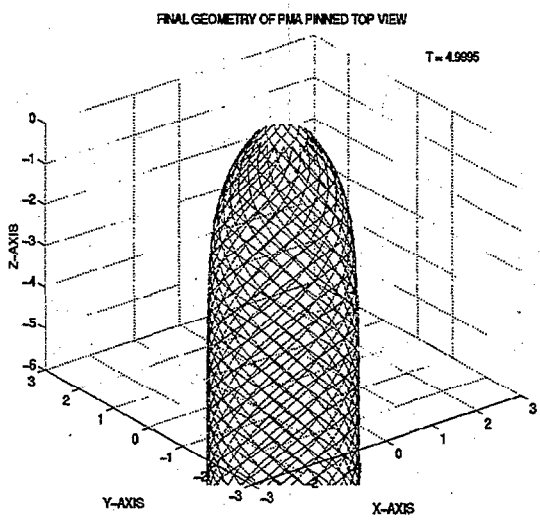

Figure 12 FEA geometry at one PMA end

These pull tests and concurrent modeling efforts should be completed during the summer of 1999. These models are expected to assist engineers in designing and utilization of PMAs. As demonstrated, end cap effects can be modeled. PMA simulations should assist in the prediction of changing material types (braid material or liner material), dimensional and scaling changes, soft-end-cap designs, maximum effective loading and the effect of over-pressure on PMA stiffness, PMA responses to limited or no internal pressure, and many other features. The TENSION9 software suite has demonstrated the ability to model PMA structures and this modeling will continue as the program develops. The software can be applied for predicting the dynamic and static behavior of many fiber reinforced membrane structures.

LARGE MUSCLE TESTING

At the time this paper is being written, a large, 6-inch-diameter PMA has been constructed for testing (Figure 13). The purpose is to demonstrate the manufacturing technology needed for large PMAs and the force generating capability needed for soft landing of vehicles. Force in excess of 100,000 lbf is expected from this test article. Tests will be conducted using a large crane at the U.S. Army Soldier Systems Center (Natick).

Figure 13 Large Muscle Test

Figure 14 contains the preliminary results of an initial slow lift experiment conducted on the 6-inch diameter PMA. The graph shows the response of the PMA length contraction as a function of the applied internal pressure for a 2100 lb payload. The initial length measured between the PMA end caps was 185 inches for this payload.

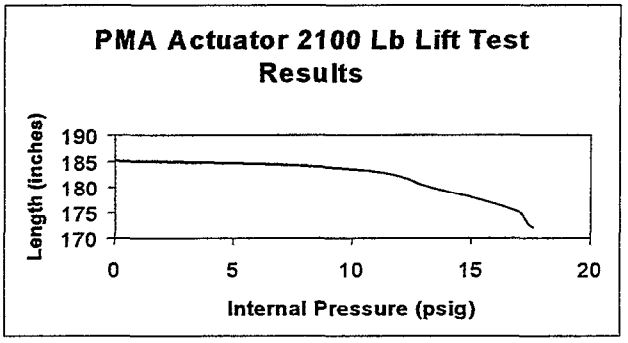

Figure 14 Preliminary Results of Lift Test

CONCLUSIONS

Pneumatic muscle actuators (PMAs) have a high potential for use in advanced recovery systems. Applications may include the following:

- Landing impact reduction for cargo and personnel;
- Parafoil steering and flare; and
- Parachute trajectory control.

A force equation has been derived for the ideal PMA and validated by static testing. Static testing also provides a measure of the efficiency of actual PMAs. Finite element analysis is being applied to develop a more general tool for predicting performance with elastic resistance and end effects.

The work reported is at an early stage. Continuing work will include correlation of measured performance with the predictions of the simulation tools under development.

REFERENCES

1. W.J. Krainski and S.E. Kunz, "The Dynamics of a Parachute Retraction Soft Landing System", Proceedings of the 14th AIAA Aerodynamic Decelerator Conference, San Francisco, CA, 1997.

2. G. Brown, R. Haggard, R. Almassy, R. Benney, S. Dellicker, "The Affordable Guided Airdrop System", Proceedings of the CEAS/AIAA 15th Aerodynamic Decelerator Systems Technology Conference, AIAA-99-1719, Toulouse, France, 1999.

3. R. J. Benney & J.W. Leonard, "A 3-D Finite Element Structural Parachute Model", Proceedings of the 13th AIAA Aerodynamic Decelerator Conference, Clearwater, FL, 1995.

4. R. J. Benney, K.R. Stein, J.W. Leonard, M.L. Accorsi, "Current 3-D Structural Dynamic Finite Element Modeling Capabilities", Proceedings of the 14th AIAA Aerodynamic Decelerator Conference, San Francisco, CA, 1997.

5. M. Accorsi, K. Lu, J. Leonard, R. Benney, K. Stein, "Issues in Parachute Structural Modeling: Damping and Wrinkling", Proceedings of the CEAS/AIAA 15th Aerodynamic Decelerator Systems Technology Conference, AIAA-99-1719, Toulouse, France, 1999.

6. R. J. Benney, K. Stein, W. Zhang, M. Accorsi, J. Leonard, "Controllable Airdrop Simulations Utilizing a 3-D Structural Dynamic Model", Proceedings of the CEAS/AIAA 15th Aerodynamic Decelerator Systems Technology Conference, AIAA-99-1727, Toulouse, France, 1999.